Design Considerations for Multi-Spectral Systems Operating in the Longwave and Midwave Bands

29 January 1998

Dr. Paul Frank Singer
Doreen M. Sasaki

Raytheon Systems Co.
EO/E1/A173
P.O. Box 902
El Segundo, CA 90245
pfsinger@mail.hac.com
310-616-1779

ABSTRACT

This paper addresses the issues associated with multi-spectral detection of small dim and CC&D targets in heavy clutter. The results are generally applicable but the examples use the infrared thermal bands because of the interest in both day and night operations. The fundamental issue which is addressed is the unknown spectral signature of the target. This problem is first addressed for the case of spectral only detection. The methodology is then extended to the case of space-spectral detection in which the spatial but not the spectral signature of the target is known. The performance loss associated with the target spectral signature being unknown is quantified in terms of increased P_{FA}.

Keywords: multi-spectral detection, space-spectral detection, thermal infrared bands, unknown spectral signature, number of spectral bands, P_{FA} performance, two color results

1. INTRODUCTION

The passive detection of small dim targets in heavy clutter is a problem within the context of many surveillance applications. These applications include airborne surveillance and reconnaissance, cruise missile defense and advance scout vehicles. Concepts of operation typically require covert operation, both day and night against CC&D targets. These requirements imply the use of the thermal infrared bands to detect targets with unknown signatures.

Robust detection of airborne targets against heavy cloud clutter has been demonstrated using space-temporal clutter rejection algorithms [1]. To realize the full potential SCR (signal-to-clutter ratio) gain of these algorithms, five to seven frames must be collected within a 500 to 750 msec. interval. These data requirements are not compatible with the required volume search rates. The volume search rates are often driven by track initiation and maintenance requirements.

Modern infrared focalplanes are able to collect data at 250 to 480 Hz. These rates support the search volume requirements but are too fast to support the needs of high gain space-temporal detection algorithms. A feasible alternative is to use the fast focalplanes to collect space-spectral data. Since spectral data should be collected as near to simultaneous as possible, this approach fully exploits modern focalplane technology. This also ameliorates some of the processing problems by providing *all* of the data immediately instead of being spread out over 500 msec. or more.

Space-spectral detection provides even greater benefits over space-temporal detection for ground based scout vehicles operating on-the-move. Collecting data on-the-move over 500 msec. presents a registration problem. Registration algorithms

REPORT DOCUMENTATION PAGE

Form Approved OMB No. 0704-0188

1. REPORT DATE (DD-MM-YYYY)	2. REPORT TYPE	3. DATES COVERED (FROM - TO)
29-01-1998	Conference Proceedings	xx-xx-1998 to xx-xx-1998

4. TITLE AND SUBTITLE
Design Considerations for Multi-Spectral Systems Operating in the Longwave and Midwave Bands
Unclassified

5a. CONTRACT NUMBER
5b. GRANT NUMBER
5c. PROGRAM ELEMENT NUMBER

6. AUTHOR(S)
Singer, Paul F. ;
Sasaki, Doreen M. ;

5d. PROJECT NUMBER
5e. TASK NUMBER
5f. WORK UNIT NUMBER

7. PERFORMING ORGANIZATION NAME AND ADDRESS
Raytheon Systems Company
EO/EI/A173
P.O. Box 902
El Segundo, CA90245

8. PERFORMING ORGANIZATION REPORT NUMBER

9. SPONSORING/MONITORING AGENCY NAME AND ADDRESS
Director, CECOM RDEC
Night Vision and Electronic Sensors Directorate, Security Team
10221 Burbeck Road
Ft. Belvoir, VA22060-5806

10. SPONSOR/MONITOR'S ACRONYM(S)
11. SPONSOR/MONITOR'S REPORT NUMBER(S)

12. DISTRIBUTION/AVAILABILITY STATEMENT
APUBLIC RELEASE
,

13. SUPPLEMENTARY NOTES
See Also ADM201041, 1998 IRIS Proceedings on CD-ROM.

14. ABSTRACT
This paper addresses the issues associated with multi-spectral detection of small dim and CC&D targets in heavy clutter. The results are generally applicable but the examples use the infrared thermal bands because of the interest in both day and night operations. The fundamental issue which is addressed is the unknown spectral signature of the target. This problem is first addressed for the case of spectral only detection. The methodology is then extended to the case of space-spectral detection in which the spatial but not the spectral signature of the target is known. The performance loss associated with the target spectral signature being unknown is quantified in terms of increased PFA.

15. SUBJECT TERMS

16. SECURITY CLASSIFICATION OF:			17. LIMITATION OF ABSTRACT	18. NUMBER OF PAGES	19. NAME OF RESPONSIBLE PERSON
a. REPORT	b. ABSTRACT	c. THIS PAGE	Public Release	11	Fenster, Lynn lfenster@dtic.mil
Unclassified	Unclassified	Unclassified			19b. TELEPHONE NUMBER International Area Code Area Code Telephone Number 703767-9007 DSN 427-9007

are computationally expensive. The registration problem for ground vehicles is exasperated by the relatively short clutter ranges. At the shorter clutter ranges, the registration error is not simply a translation or even a translation and rotation of the scene, it is optical flow. Algorithms which correct the optical flow exist but, they too are computationally expensive and the results are not completely satisfying. The ability to collect spectral data rapidly avoids the costs and problems of optical flow.

Space-spectral detection solves several important system design issues associated with space-temporal detection if the necessary SCR gain can be attained. The fundamental issue in realizing that gain is the unknown target spectral signature. In the thermal infrared bands the spectral signature of the target is highly variable because of its dependence upon aspect angle, recent operating history, surface characteristics (clean, dusty, wet, etc.), spectral coloration of the atmosphere and variations in reflected radiance (e.g. cloud cover variations). The target signature problem is even worse for a CC&D target because it has been intentionally altered to be more clutter like. The next section of this paper addresses the effect or more specifically the performance loss resulting from the target spectral signature being unknown. The analysis proceeds from the spectral only case to the case of interest, space-spectral detection. Section 3 presents the results of spectral only detection for a two color (midwave and longwave) system. The same two color data is processed in Section 0 with the space-spectral algorithm developed in Section 2 for the case of the unknown spectral signature.

2. SIGNAL PROCESSING

The quintessential performance metrics of a detection system are the probability of detection (P_D) and the false alarm probability (P_{FA}). The relationship between these two metrics is characterized by the ROC (receiver operating characteristic) curve. The ROC curve is a plot of P_D versus P_{FA} and is parameterized by the detection threshold τ.

To construct the ROC curve, the probabilities of detection and false alarm must be evaluated. Let $y = u + v$ be the input to the detection operation where u and v are the target and clutter responses of the system respectively. The probability of false alarm is the probability that the clutter v exceeds the detection threshold τ,

$$(1) \qquad P_{FA} = P\{v > \tau\} = \int_{\tau}^{\infty} f_v(v)\, dv$$

where $f_v(v)$ is the probability density function of v. Without loss of generality, assume v is zero mean, then define a new random variable $\theta = v/\sigma_v$ which has unit variance. The probability density function of this normalized random variable can be expressed in terms of the probability density function of v as follows:

$$(2) \qquad f_\theta(\theta) = \sigma_v\, f_v(\sigma_v \theta)$$

Now perform the indicated change of variable on Eq.(1).

$$(3) \qquad P_{FA} = \sigma_v \int_{\tau/\sigma_v}^{\infty} f_v(\sigma_v \theta)\, d\theta = \int_{\tau/\sigma_v}^{\infty} f_\theta(\theta)\, d\theta$$

The probability of detection is the probability that y exceeds the detection threshold τ when a target is present $(u \neq 0)$.

$$(4) \qquad P_D = P\{y > \tau\} = P\{v > \tau - u\}$$

From the preceding analysis it follows that

$$(5) \qquad P_D = \sigma_v \int_{\tau-u}^{\infty} f_v(v)\, dv = \int_{\tau/\sigma_v - SCR}^{\infty} f_\theta(\theta)\, d\theta$$

where the signal-to-clutter ratio (SCR) is defined to be u/σ_v .

Observe that the expressions for P_D and P_{FA} are the same except for the appearance of the SCR in the expression for P_D. By definition the probability density function $f_\theta(\theta)$ is non-negative, hence P_D is and increasing function of SCR and P_D will be maximized by maximizing the SCR.

The SCR can be maximized by applying a matched filter to the data prior to the detection operation. Specifically, the matched filter is the linear filter designed to maximize the SCR. Its general form is

$$(6) \qquad y = \left(\vec{s}^{\,t} \Sigma_x^{-1}\right)\left(a\vec{s} + \vec{x}\right) = u + v$$

where

$a\vec{s}+\vec{x}=$ the input to the filter.

$a\vec{s}=$ the assumed known form of the target signal where *a* is the unknown signal amplitude.

$\vec{x}=$ the clutter plus noise.

$\left(\vec{s}^{\,t}\Sigma_x^{-1}\right)=$ the impulse response of the matched filter.

$\Sigma_x=$ the clutter plus noise covariance matrix.

$= E\left\{\vec{x}\,\vec{x}^{\,t}\right\}$

$y=$ the output of the matched filter and the input to the detection threshold.

$u=$ the target response of the matched filter.

$= a\vec{s}^{\,t}\Sigma_x^{-1}\vec{s}$

$v=$ the clutter plus noise response of the matched filter.

$= \vec{s}^{\,t}\Sigma_x^{-1}\vec{x}$

$\sigma_v^2 = \vec{s}^{\,t}\Sigma_x^{-1}\vec{s}$

The SCR at the output of the matched filter can be calculated from the definition.

$$(7)\qquad SCR=\frac{u}{\sigma_v}=a\sqrt{\vec{s}^{\,t}\Sigma_x^{-1}\vec{s}}$$

It is of interest to note that the matched filter and the above results are independent of the clutter distribution - no Gaussian assumption was necessary.

The general form of the matched filter given above can be applied to data in any domain or combination of domains. It was applied in the spatial domain for Shipboard IRST cruise missile defense [2]. The AIRMS program applied it to the space-temporal domain for long range detection of small dim targets in heavy clutter [3]. Section 3 applies the matched filter to the spectral domain and Section 0 extends it to the space-spectral domain.

A fundamental assumption of the matched filter is that $\vec{s}$, the form of the target signal, is known to within a multiplicative constant (*a*). This assumption is readily satisfied in the spatial domain for unresolved targets. In this case the spatial shape (form) of the target is the sensor point spread function. In the temporal domain the target is assumed to have constant velocity during the observation interval and a bank of velocity filters is implemented [4]. Unfortunately no such assumptions about the spectral signature of the target are generally valid. The spectral signature of the target depends upon the aspect angle (even if unresolved), operating history, cleanliness and prevailing atmospheric conditions.

In the absence of knowledge about the spectral signature of the target, the matched filter formulation can still be used albeit with reduced performance. How the spectral signature is used by the matched filter and the corresponding performance loss can be obtained from an eigen-analysis of the matched filter.

The general form of the matched filter when applied in the spectral domain is

$$(8)\qquad y=\vec{b}^{\,t}\Sigma_\lambda^{-1}\vec{x}$$

where

$\vec{b}=$ the spectral signature of the target.

$\Sigma_\lambda=$ the spectral covariance of the clutter.

and $\vec{x}$ is a sample of clutter to be spectrally filtered.

Since the spectral covariance is positive definite, it can be factored as follows.

$$(9)\qquad \Sigma_\lambda = V\Lambda_\lambda V^t = V\Lambda_\lambda^{1/2}\Lambda_\lambda^{t/2}V^t$$

The matrix V formed from the eigenvectors of Σ_λ is a unitary transformation. The eigenvalue matrix Λ_λ is diagonal with the diagonal elements (eigenvalues) being the clutter power (variance) in the corresponding eigen-directions. The matched filter in Eq. (8) can now be expressed in the following form.

$$(10)\qquad y = \left[\vec{b}^{t} V \Lambda_{\lambda}^{-t/2}\right]\left[\Lambda_{\lambda}^{-1/2} V^{t} \vec{x}\right] = \vec{b}'^{t}\vec{x}'$$

The vector $\vec{x}'$ is obtained by using V to transform $\vec{x}$ into the principle coordinate system of the eigenvectors. The elements of the transformed vector are uncorrelated. The matrix $\Lambda_{\lambda}^{-1/2}$ then scales the transformed vector so that all the elements of $\vec{x}'$ have unit variance. The vector $\vec{b}'$ is obtained from $\vec{b}$ by the same sequence of transformations. Figure 2-1 depicts this process in two spectral dimensions.

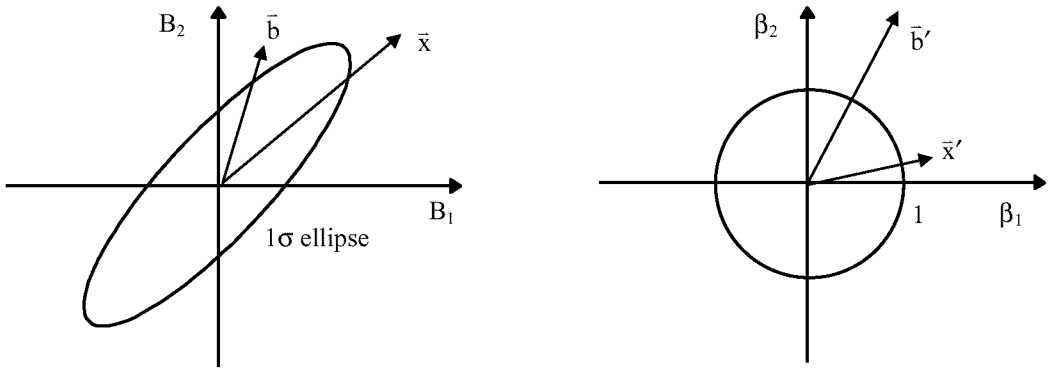

Figure 2-1 Rotation and scaling performed by the matched filter.

When viewed in the rotated and scaled domain, the matched filter output is simply the projection of the data (both target and clutter) onto the $\vec{b}'$ vector. If the projection is greater than the detection threshold τ, then a detection is declared. Clearly, a target vector $a\vec{b}'$ would project onto $\vec{b}'$ without any loss. This process is shown in Figure 2-2. Notice that even though the length of the clutter vector $\vec{x}'$ is greater than the threshold, its projection onto $\vec{b}'$ is not hence, it would *not* give rise to a false alarm.

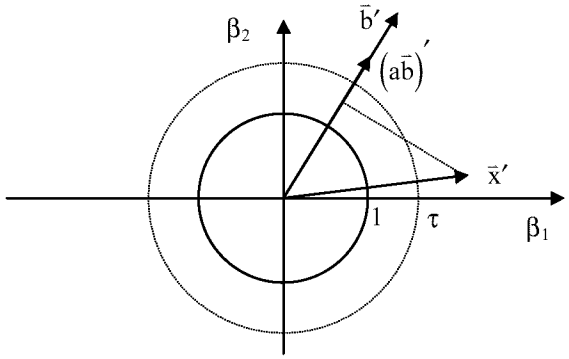

Figure 2-2 Matched filter processing in the rotated and scaled domain.

If the spectral signature $\vec{b}$ of the target is unknown, then any vector of length τ or greater in the rotated and scaled space of the matched filter would be a detection. That is, any vector $\vec{x}'$ outside the circle of radius τ would be detected. The false alarm performance of such a detector will clearly be inferior to the matched filter.[†]

The increase in P_{FA} is easily quantified and provides some insight into how the number of spectral bands, N_{λ}, affects performance.

[†] The detection performance will improve slightly for weak targets but, on the basis of a ROC curve comparison, performance overall will be lost.

(11) $P_{FA} = P\{|\vec{x}'| > \tau\} = P\{|\vec{x}'|^2 > \tau^2\}$

If it is assumed that the underlying distribution of the clutter $\vec{x}$ is Gaussian, then $|\vec{x}'|^2$ is χ^2 distributed and

(12) $P_{FA} = \int_{\tau^2}^{\infty} f_{\chi^2}(\theta; N_\lambda)\, d\theta$

where $f_{\chi^2}(\theta; N_\lambda)$ is the χ^2 distribution with N_λ degrees of freedom. Figure is a plot of P_{FA} as a function of τ for various numbers of spectral bands.

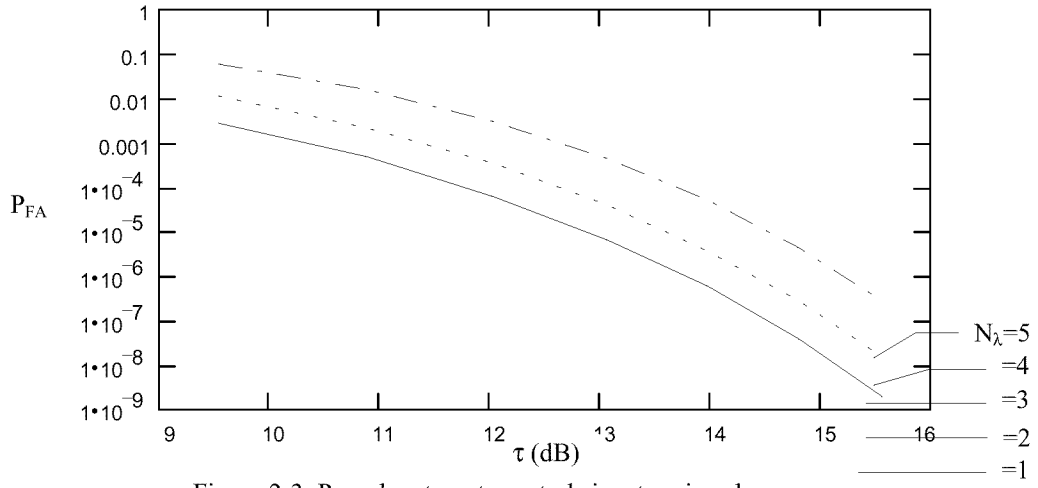

Figure 2-3 P_{FA} when target spectral signature is unknown.

Observe that additional spectral bands increase the P_{FA} and hence should only be included if there is a commensurate increase in P_D which improves ROC performance.

If the domain of the measurements is mixed, for example space-spectral, then $\vec{s}$ will be partially known. Presumably the point spread function $\vec{s}_k$ of the k-th spectral band will be known but, the spectral signature of the target will remain unknown. It will now be shown how the previous method for an unknown target signature can be extended to the mixed domain case .

The matched filter for space-spectral data has the following form.

(13) $y = \left(b_1 \vec{s}_1^{\,t} \;\middle|\; b_2 \vec{s}_2^{\,t} \;\middle|\; \cdots \;\middle|\; b_{N_\lambda} \vec{s}_{N_\lambda}^{\,t} \right) \Sigma_x^{-1} \vec{x}$

The unknown spectral signature $\vec{b}$ can be factored out as follows.

(14) $$y = \begin{pmatrix} b_1 & b_2 & \cdots & b_{N_\lambda} \end{pmatrix} \begin{pmatrix} \vec{s}_1^{\,t} & 0 & \cdots & 0 \\ 0 & \vec{s}_2^{\,t} & \cdots & 0 \\ \vdots & \vdots & \ddots & \vdots \\ 0 & 0 & \vdots & \vec{s}_{N_\lambda}^{\,t} \end{pmatrix} \Sigma_x^{-1} \vec{x}$$

$$= \vec{b}^{\,t} S^t \Sigma_x^{-1} \vec{x}$$

Now define the random vector $\vec{z}$ with dimension N_λ .

(15) $\vec{z} = S^t \Sigma_x^{-1} \vec{x}$

The covariance matrix of $\vec{z}$, derived below is $N_\lambda \times N_\lambda$ dimensional

(16) $\Sigma_z = E\{\vec{z}\,\vec{z}^{\,t}\} = S^t \Sigma_x^{-1} S$

and can be factored as before.

(17) $\Sigma_z = V_z \Lambda_z^{1/2} \Lambda_z^{t/2} V^t$

The space defined by $\vec{z}'$ below

(18) $\vec{z}' = \Lambda_z^{-1/2} V_z^t \vec{z}$

has the same characteristics as the $\vec{x}'$ space defined in Eq. (10); the elements of $\vec{z}'$ have unit variance and are uncorrelated. In the space of $\vec{z}'$, the matched filter can be expressed as the projection of $\vec{z}'$ onto the transformed target spectral vector.

(19) $y = \left[\vec{b}^t V_z \Lambda_z^{1/2}\right] \vec{z}$

If the target spectral signature $\vec{b}$ is unknown, then detection can be accomplished as in the spectral domain.

(20) Declare a detection if: $|\vec{z}'| > \tau$

The concept of defining the detection process in the domain of $\vec{x}'$ (spectral) or $\vec{z}'$ (space-spectral) can be generalized by defining a detection function $D(\vec{z}';\tau)$.

(21) Declare a detection if: $D(\vec{z}';\tau) > 0$

This formulation admits the use of partial knowledge of the target signature. Returning to the example in Figure 2-2, if it has been determined that the spectral response of the target is greater in band b_2 than in band b_1, then the constraint $(b_2 > b_1)$ can be transformed into the domain of $\vec{x}'$ and the detection region can be restricted as shown in 2.4. The inclusion of the constraint $(b_2 > b_1)$ effectively reduces P_{FA} by a factor of two with little impact on P_D.

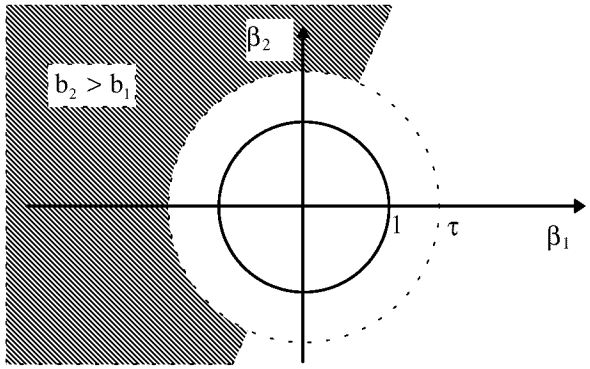

Figure 2-4 Detection region constrained by partial knowledge of the target signature.

In general spectral constraints of the form

(22) $\vec{a}^t \vec{b} > c$

are easily included in the detection function $D(\cdot;\tau)$ by transforming them into the domain of the detection function.

(23) $\left(\vec{a}^t V \Lambda^{1/2}\right)\left(\Lambda^{-1/2} V^t \vec{b}\right) > c$

The detection scheme described above in which no target signature information is used is anomaly detection. That is, detections are being declared because they are not clutter like. The detection function then dichotomizes the detection space into two mutually exclusive regions, clutter and not-clutter. Only the elements of the not-clutter region are further considered. A high P_D then implies a large not-clutter region and a lot of false detects that need to be eliminated. The use of spectral constraints helps to reduce the number of false detects which require additional processing.

3. SPECTRAL PROCESSING

Figure 3-1 is a block diagram of a matched filter based spectral processing paradigm. The input to the paradigm is a stack of n frames from a set of n spectral bands. Prior to the clutter filter, the data are spatially demeaned. This demeaning

process acts as a high pass filter and is intended to reject any low frequency clutter. The residual high frequency clutter which typically competes with the target signal is rejected by the matched filter. The demeaning operation is performed spatially only because of the spectral dependence of the mean.

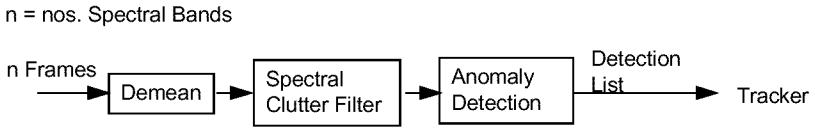

Figure 3-1 - Spectral Processing Block Diagram

The spectral clutter rejection filter is based on the matched filter which is designed to optimally reject clutter while enhancing the target response to the filter. The matched filter based clutter rejection filter has two components, the inverse spectral covariance and the spectral target template.

The inverse spectral covariance is estimated by the inverse of the sample spectral covariance matrix which is constructed using a fully adaptive approach. To be fully adaptive, the sample covariance is calculated from the volume of data to be filtered. The data volume is composed of the stack of n spatially demeaned frames. A sample vector is formed by extracting a one dimensional spectral block of pixels from the data volume and lexiographically ordering it. A sequence of sample vectors is formed by extracting successive blocks of pixels from the data volume. The sample covariance is

$$(24) \qquad S_x = \frac{1}{M}\sum_{k=0}^{M-1} \vec{x}_k \vec{x}_k{}^T$$

where $\vec{x}_k$ is one of the M sample vectors.

The block of pixels is referred to as the covariance window. For spectral only processing, the size of the covariance window is 1 pixel in both azimuth and elevation, and n pixels in the spectral dimension. The number of samples used to estimate the sample covariance matrix typically is large enough to achieve a statistical sample and still be practical. The matched filter is applied to the same data from which the filter was designed. This is referred to as "self-whitening" [5] and is a robust and effective method of clutter rejection.

From the previous section, the spectral clutter rejection filter can be viewed as an inner product of two linearly transformed vectors. The operator $\Lambda_\lambda^{-1/2} V^t$ whitens the data by rotating the clutter and target data onto the eigenvectors and inversely scaling the axes of the new space by the clutter standard deviations as shown in Figure 2-1. The same operator transforms the target template into the whitened space. The spectral target template is the amplitude of the target signal in each of the spectral bands. The matched filter is the projection of the data onto the spectral target template in the whitened space.

Typically the target spectral signature is unknown and the projection is precluded. Alternatively, anomaly detection determines detections by the length of the whitened vectors. The length of the target vector in the whitened space can be considered as an estimate of the SCR. Whitened vectors which have length greater than a predetermined threshold are declared detections.

The spectral only processing paradigm was applied to actual data collected by the AADEOS system [6], a simultaneous two color system which operates in the 3.8 - 5.1 and 7.9 - 10.2 μm spectral bands. Each frame was initially cropped to a size of 208 pixels in azimuth and 128 pixels in elevation. The midwave IR (MWIR) frames are offset from the longwave IR (LWIR) frames by 74 pixels therefore, the frames were further cropped to render frames which were 134 pixels in azimuth.

Figure 3-2 shows samples of an MWIR frame and the corresponding LWIR frame. This test data set contains a single UH-1 helicopter target at a range estimated by NVESD to be approximately 5 km. No ground truth data is available for this data set. The helicopter orientation is a frontal aspect. The helicopter target is assumed to be unresolved in both bands and subtends at most two pixels. Estimates for the input SCR for the MWIR and LWIR bands are 0.1 dB and -6.8 dB respectively. The spectral correlation coefficients estimated from the data are approximately .96 in the sky region and .92 in the clutter region. The AADEOS sensor was mounted on a tripod therefore full stabilization is assumed.

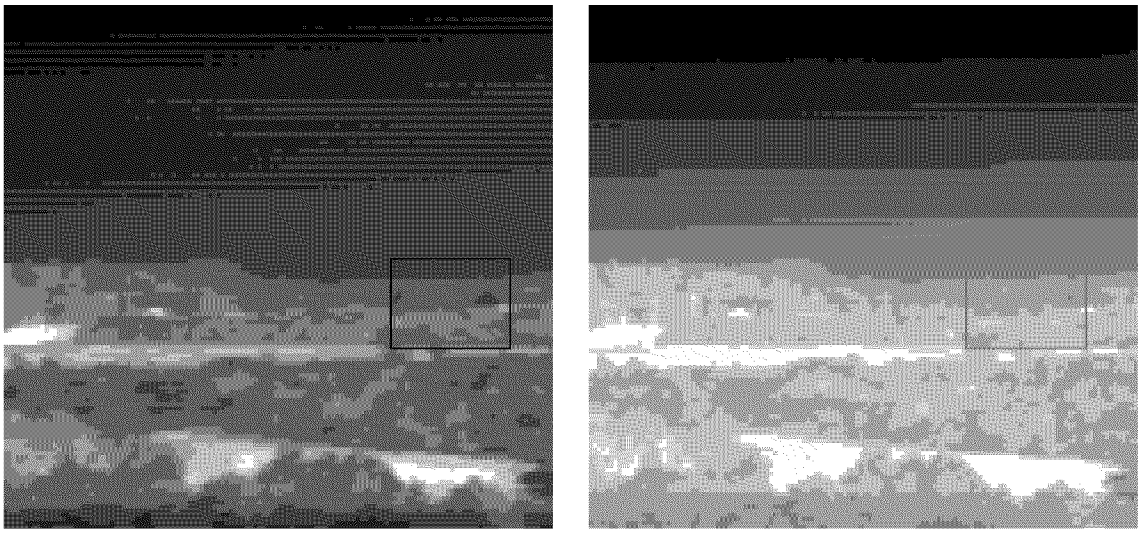

MWIR **LWIR**

Figure 3-2 Sample frames of Midwave and Longwave IR Data

The spectral only paradigm was applied to the test data set. Prior to applying the paradigm, row means were removed from the data to mitigate sensor pattern noise which is typical of scanning systems. A scatterplot of the row demeaned MWIR data versus the row demeaned LWIR data (Figure 3-3) illustrates the spectral relationship of the data. The spectral correlation of the clutter is evident from the angle between the MWIR axis and the principle axis indicated by ε_1. A data point in the scatterplot corresponds to the endpoint of a spectral vector. The target vector is positioned amid the clutter points. Prior to the clutter rejection filter, a spatial demeaning filter was applied. The spatial demeaning operation can be viewed as a translation of the coordinate system to the center of the clutter ellipse.

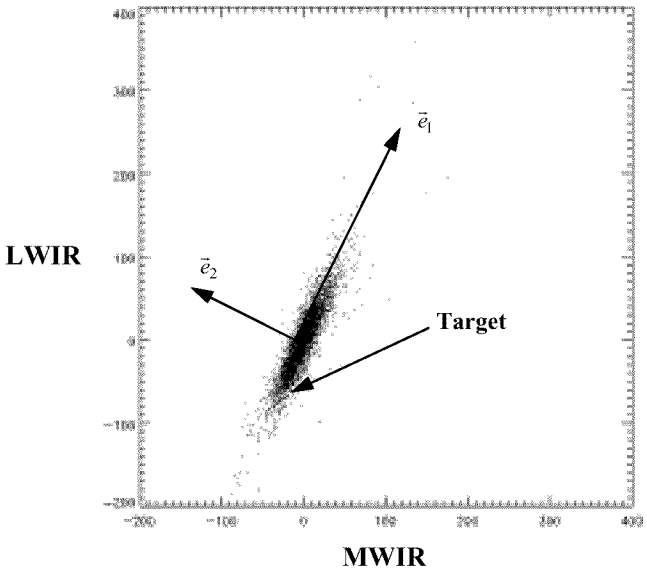

Figure 3-3 Dual Band data after the Row Demeaning

Figure 3-4 shows the data in the whitened space. The scatterplot of the whitened clutter data is circular in shape indicating no perceptible spectral correlation. The target vector is still within the clutter. Anomaly detection was performed on the spectrally whitened data. Data points lying outside the circular threshold are considered a detection (Figure 3-4). For

this test data set, the target SCR after spectral only processing is 2.8 dB. If the detection threshold is set at the target SCR, then the corresponding probability of false alarm is 0.271. Parameters used for processing appear in Table 4-1.

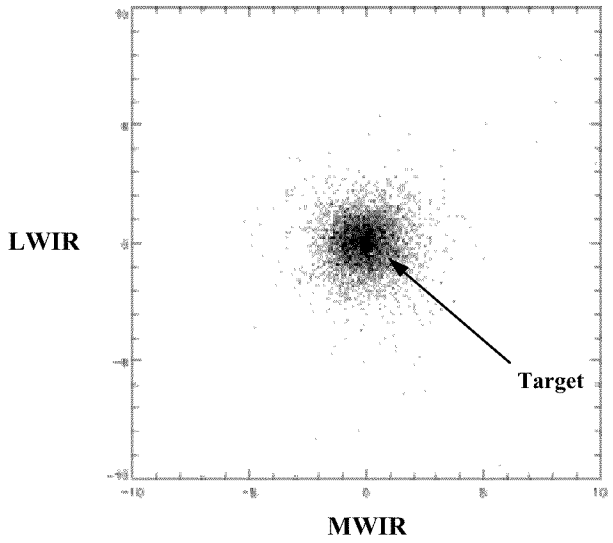

Figure 3-4 Scatterplot after Spectral Whitening Filter

Spectral only processing provides limited performance improvement. A relatively low threshold is needed to detect the target. The corresponding false alarm rate will overwhelm even the most sophisticated tracker. Moreover, single band fully adaptive spatial processing is expected to out perform spectral only processing. A matched filter based fully adaptive 2D spatial filter was applied to the test data. The MWIR SCR and LWIR SCR from a local CFAR detector are 13.1 dB and 10.9 dB respectively. The corresponding probabilities of false alarm are respectively 9.2×10^{-4} and 4.9×10^{-3} for the MWIR and LWIR bands. Parameters used for processing appear in Table 4-1.

4. SPACE - SPECTRAL PROCESSING

The motivation for coupled space spectral processing is to improve clutter rejection performance by exploiting the spatial and spectral dimensions. A block diagram of the coupled space spectral paradigm appears in Figure 4-1. As in spectral processing, the data is first spatially demeaned. The space spectral clutter rejection filter as described in Section 0 is based on the matched filter and consists of an inverse covariance and space spectral target template. Because the target template is only partially known, the clutter rejection filter is followed by an anomaly detection scheme.

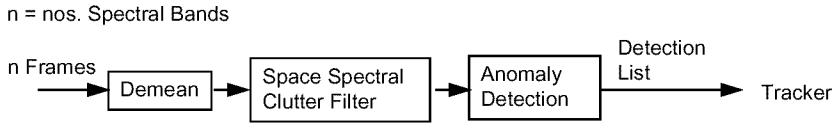

Figure 4-1 Coupled Space Spectral Paradigm

The coupled paradigm is based on a fully adaptive matched filter approach. As before, the estimator for the covariance matrix is the sample covariance which is computed from the data. The sample vectors are extracted from a three dimensional block of pixels of the space spectral data volume and lexiographiclly ordered. A sequence of sample vectors is formed from successive blocks of pixels and a sample covariance is computed using Eq.(24). The spatially demeaned data are "self-whitened" using the inverse sample covariance matrix which was built from space *and* spectral data samples. The target template spans both the spatial and spectral domains. The known spatial target template is taken to be the sensor point spread function which is consistent with the premise of unresolved targets. Compensation for the unknown spectral target template is achieved through anomaly detection.

The coupled paradigm was applied to the row demeaned AADEOS test data set. The coupled space spectral signal processing parameter settings are summarized in Table 4-1. The size of the demeaning window was 23 pixels in azimuth, and

3 pixels in elevation. The size of the covariance windows used to estimate the sample covariance was 5 pixels in azimuth, 7 pixels in elevation, and 2 pixels in the spectral dimension. MWIR and LWIR sensor point spread functions were modeled from AADEOS the sensor parameters and were used as the spatial target templates. The whitened data was projected onto the spatial target templates. Anomaly detection was performed in the spectral domain.

The coupled space spectral paradigm out performed the spectral only and spatial only processing. The scatterplot in Figure 4-2 clearly shows the superior performance of the whitening filter. The length of the whitened target vector exceeds those of the whitened clutter vectors. The SCR was 15.5 dB and the corresponding probability of false alarm was 1.5E-4. The performance gain of the coupled processing over single domain processing is attributed to improved clutter rejection from the additional domain.

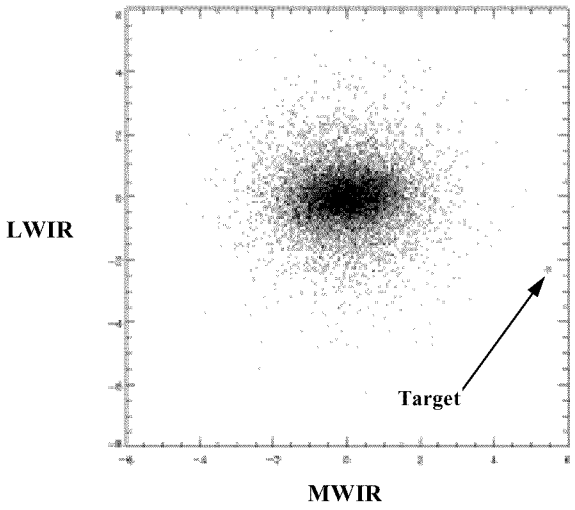

Figure 4-2 Scatterplot after Coupled Space Spectral Whitening Filter

Parameter	*Dual Band Spectral Only*	*Single Band Spatial Only*	*Dual Band Coupled Space Spectral*
Demeaning Window (azimuth x elevation x spectral band)	23 x 3 x 1	23 x 3 x 1	23 x 3 x 1
Covariance Window (azimuth x elevation x spectral band)	1 x 1 x 2	5 x 7 x 1	5 x 7 x 2
Sensor Point Spread Function (azimuth x elevation)	5 x 7	5 x 7	5 x 7

Table 4-1 - Signal Processing Parameters

5. CONCLUSIONS

Multi-spectral processing is suited for scenarios in which the natural terrain and deceptive techniques deny adequate single band signal-to-clutter ratio. Typical scenarios for scout vehicles include helicopters hovering at and against the treeline and military vehicles against terrain or forested regions. Modern focal plane technology can provide acceptable multi-spectral data. Algorithms which exploit the spatial and spectral domains are an enabling technology for airborne surveillance and on-the-move land based systems.

A fully adaptive matched filter based coupled space spectral paradigm is a feasible multi-spectral processing scheme. The strong analytical foundation enables performance prediction and demonstrates depth of understanding. Substantial performance gain was demonstrated on broad band two color data from an actual land based system in a CC&D situation. A

multi-spectral system concept based on the coupled space spectral paradigm has been defined. Airborne performance estimates will be available after validation on actual data.

Preliminary estimates indicate no significant increase (and maybe even a slight decrease) in computations per pixel for the fully adaptive space spectral filter followed by anomaly detection when compared to single band spatial only processing involving a CFAR detector. Anomaly detection requires considerably less computations than implementation of a CFAR detector. Consequently, multi-spectral processing affords future scout vehicles with real-time processing and an on-the-move capability against CC&D threats.

REFERENCES

1 Attili, J.B., Blackman, S.S., Chan, C.L., Dempster, R.J., Henderson, P. and Singer, P.F., "Characterization and Mitigation of False Tracks in a 3D Signal Processor," Proc. of Signal and Data Processing of Small Targets 1996, O.E. Drummond (ed.), vol. 2759, SPIE, Orlando FL, Apr 1996.

2 Buss, J., Barnett, J., Floren, E., Klausen, M., Metcalf, T., Ricks, R., Singer, P., Blackman, S. and Sasaki, D., "Analysis and Demonstration of Shipboard IRST Signal Processing and Tracking," IRIS TBD, Monterey, CA, Feb. 1997.

3 Attili, J.B., Blackman, S.S., Chan, C.L., Dempster, R.J., Henderson, P. and Singer, P.F., "Characterization and Mitigation of False Tracks in a 3D Signal Processor," Proc. of Signal and Data Processing of Small Targets 1996, O.E. Drummond (ed.), vol. 2759, SPIE, Orlando FL, Apr 1996.

4 Singer, P.F., "Performance Analysis of a Velocity Filter Bank," Proc. of Signal and Data Processing of Small Targets 1997, O.E. Drummond (ed.), vol. 3163, pp. 96-107, SPIE, San Diego CA, Jul 1997.

5 Singer, P.F. and Sasaki, D.M., "Analysis of Target Capture Loss for Fully Adaptive Matched Filters," Proc. of Signal and Data Processing of Small Targets 1996, O.E. Drummond (ed.), vol. 2759, SPIE, Orlando FL, Apr 1996.

6 Carr, T., Rothstein, D. And Teti, C., "Advanced Air Defense Electro-Optical Sensor (AADEOS) Final Report," Doc. No. 34040-002, NVESD, Fort Belvoir,VA, Oct. 1994.